Two-Mode Squeezing and the EPR Paradox: On The Fundamentality and Applications of Quantum Correlations

Ben Knepper[1, *]
(PHYS 130: Quantum and Nonlinear Optics)
[1] *Department of Physics, University of California, Berkeley, California 94720, USA*

(Dated: May 9, 2024)

"Squeezed light" refers to non-classical states of the electromagnetic field in which the noise at some phases is less than the noise of the vacuum state. These bewildering states manipulate fundamental limits set by quantum mechanics and results in correlations between phases either at the same mode frequency, or across two different mode frequencies. The EPR Paradox refers to the puzzling property of quantum mechanics that for two particles which are entangled, or strongly correlated, the physical state of one particle can be influenced by a measurement on the other. As will be demonstrated, the strange quantum correlations present in both two-mode squeezed states and the EPR paradox have a deep connection: the latter can be interpreted as a limiting case of the former in which the degree of squeezing approaches infinity. Applications of this connection to enhancing quantum sensing efficiency in LIGO are subsequently discussed.

I. SQUEEZED LIGHT

Quantum optics has discovered a myriad of non-classical states which the electromagnetic field can occupy, one of which being the so-called "squeezed state" [1]. In general, the notion of a squeezed state simply refers to a particular relationship between two non-commuting observables of a physical state $\hat{A}, \hat{B}$ where $[A, B] = i\hat{C}$. A fundamental limit set by quantum mechanics is the general Heisenberg Uncertainty Principle (HUP) which these operators must obey [2]:

$$\langle(\Delta\hat{A})^2\rangle\langle(\Delta\hat{B})^2\rangle \geq \frac{1}{4}|\langle\hat{C}\rangle|^2 \tag{1}$$

Squeezed states denote states in which either $\hat{A}$ or $\hat{B}$ have an uncertainty that is less than the lower limit of the HUP. These observables could range from position and momentum to the quadratures of an electromagnetic field. Squeezed states, therefore, have useful applications to high precision measurements of an observable, such as in quantum communication and quantum sensing [2]. In the context of quantum optics specifically, squeezing can occur within a single electromagnetic mode or across multiple modes, which we now discuss in more detail.

A. Single-Mode Squeezing

Consider first a single-mode electromagnetic field. Using the standard second quantization procedure, we can parameterize the electromagnetic states by photon creation (raising) and annihilation (lowering) operators, $\hat{a}^\dagger$ and $\hat{a}$, and define any arbitrary quadrature of the electromagnetic field as

$$\hat{Y}(\theta) = \frac{1}{2}(\hat{a}e^{i\theta} + \hat{a}^\dagger e^{-i\theta}) \tag{2}$$

Note that when $\theta = 0$ and $\theta = \pi$, one recovers the familiar real and imaginary quadratures, analogous to position and momentum of the harmonic oscillator:

$$\hat{X}_1 = \hat{Y}(\theta = 0) = \frac{1}{2}(\hat{a} + \hat{a}^\dagger) \tag{3}$$

$$\hat{X}_2 = \hat{Y}(\theta = \pi) = \frac{1}{2i}(\hat{a} - \hat{a}^\dagger) \tag{4}$$

Alternatively, one can attain the amplitude and phase quadratures of the single-mode field with frequency w by choosing $\theta/2 = wt$. Due to the anti-commutation relation $\left[\hat{a}, \hat{a}^\dagger\right] = 1$ the HUP uncertainty relation between any two orthogonal quadratures is

$$\langle(\Delta\hat{X}_1)^2\rangle\langle(\Delta\hat{X}_2)^2\rangle \geq \frac{1}{16} \tag{5}$$

Notably, the vacuum state $|0\rangle$, the state with no photons, minimizes this uncertainty product: $\langle 0|(\Delta\hat{Y})^2|0\rangle = 1/4$. Squeezed states, therefore, are states in which one quadrature exhibits less noise fluctuations than vacuum state [2].

A squeezed state $|\psi_{sq}\rangle = \hat{S}\,|\psi\rangle$ is obtained from the "squeezing operator"

$$\hat{S}(r, \theta) = \exp\left\{\frac{1}{2}\Big(\xi^*\hat{a}^2 - \xi\hat{a}^{\dagger 2}\Big)\right\} \tag{6}$$

where $\xi = re^{i\theta}$ quantifies both the degree of squeezing r known as the squeezing parameter, and the direction of squeezing along the quadrature $\hat{Y}(\theta)$. Single-mode squeezing is often called quadrature squeezing for this reason.

To demonstrate how the squeezing operator reduces uncertainty in one quadrature, let us consider its action on the single-mode vacuum state $\hat{S}\,|0\rangle$. Here we take $\theta = 0$ for convenience. To calculate the resulting variance in $\hat{X}_1$, one needs to calculate expectation values of $\hat{a}$ and $\hat{a}^\dagger$ with respect to the squeezed vacuum. Using

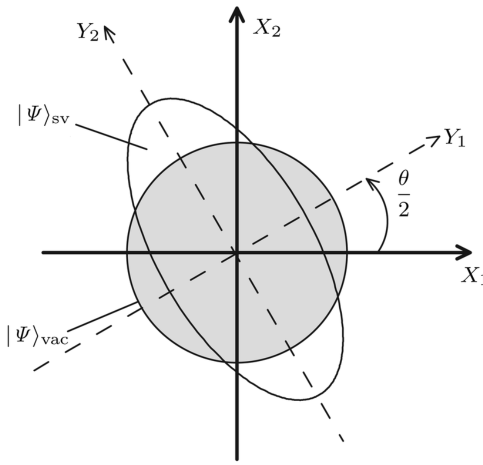

Figure 1. Phase space diagram of single-mode squeezed vacuum. Middle circle is unsqueezed vacuum, and ellipse shows squeezing in the amplitude quadrature and anti-squeezing in the phase quadrature [3].

the Baker-Hausdorff Lemma [2], these operators transform according to

$$\hat{S}^\dagger \hat{a} \hat{S} = \hat{a} \cosh r - \hat{a}^\dagger \sinh r \tag{7}$$

$$\hat{S}^\dagger \hat{a}^\dagger \hat{S} = \hat{a}^\dagger \cosh r - \hat{a} \sinh r \tag{8}$$

known as the "Bogoliubov transformation" [4].

Applying the same procedure to $\hat{X}_2$, we arrive at the variances

$$\langle(\Delta \hat{X}_1)^2\rangle = \frac{1}{4} e^{-2r} \tag{9}$$

$$\langle(\Delta \hat{X}_2)^2\rangle = \frac{1}{4} e^{2r} \tag{10}$$

which demonstrates squeezing by a factor of $\exp(-2r)$ in $\hat{X}_1$ and anti-squeezing by $\exp(2r)$ in $\hat{X}_2$ [2]. Figure 1 shows squeezed vacuum for the general case of $\theta \neq 0$.

The physical significance of the squeezing operator and the Bogoliubov transformations can be understood from two considerations. First, from eq. 6 one can see that the photon creation and annihilation operators are quadratic, implying that squeezing acts on photons in pairs. In fact, one of the first formulations of squeezed states referred to them as "two-photon coherent states" [5, 6] which obey the linear transformations

$$\hat{b} = \mu \hat{a} + \nu \hat{a}^\dagger, \tag{11}$$

$$|\mu^2| - |\nu^2| = 1 \tag{12}$$

Note that setting $\hat{b} = \hat{a}, \mu = \cosh r$, and $\nu = \sinh r$ is a valid solution and recovers the squeezed state Bogoliubov transformations of eqs. 7, 8. This demonstrates that $\hat{S}\,|0\rangle$ is the two-photon coherent state between the vacuum and itself.

Second, because the squeezing operator is unitary, it can be interpreted as a dynamical time-evolution operator of a Hamiltonian of the form

$$\hat{H} = \frac{i\hbar\chi^{(2)}}{2}\left(\hat{a}^2 - \hat{a}^{\dagger 2}\right) \tag{13}$$

such that $\hat{S}(\xi) = \hat{U}(t,0) = \exp\left(-i\hat{H}t/\hbar\right)$ with $\xi = 2\chi^{(2)}t$ [2, 4]. Interestingly, this squeezing Hamiltonian is precisely equivalent to the Hamiltonian of spontaneous parametric down-conversion in a $\chi^{(2)}$ crystal, when treated in the interaction picture. The classical nonlinear Maxwell equations describing the degenerate parametric amplifier are

$$\frac{\partial \tilde{E}_1}{\partial z} = \frac{i w_1^2 \chi^{(2)}}{4 k_1 c^2} \tilde{E}_1 \tilde{E}_2^* e^{i\Delta k z} \tag{14}$$

where k_1, w_1 is the signal wave vector and frequency, $\Delta k = k_3 - k_2 - k_1$, c is the speed of light and $\tilde{E}_1, \tilde{E}_3$ are the signal and pump beams and $\tilde{E}_2 = \frac{1}{2}\tilde{E}_1$ for degenerate parametric amplification [7]. The solutions these equations have the form

$$\tilde{E}_1 = A \cosh(\kappa z) + B \sinh(\kappa z). \tag{15}$$

which take the same general form as the Bogoliubov transformations.

Therefore, we can view a single-mode squeezed state as the signal beam produced in the $\chi^{(2)}$ nonlinear optical process of degenerate parametric amplification. The Bogoliubov transformations when viewed in the Heisenberg picture provides the corresponding dynamical evolution of the mode operators $\hat{a}$ and $\hat{a}^\dagger$ from this three-wave mixing process. This very method has been used to produce squeezed light in a variety of experiments [4]. It is worth mentioning that squeezed light has also been produced by other nonlinear mechanisms such as four-wave mixing in $\chi^{(3)}$ materials [8].

B. Two-Mode Squeezing

Two-mode squeezing is an extension of single-mode squeezing to creation and annihilation operators across different field modes. Consider two different mode operators $\hat{a}$ and $\hat{b}$, which obey the standard commutation relation $\left[\hat{a}, \hat{b}^\dagger\right] = 0$. The two-mode squeezing operator is then defined as [2]

$$\hat{S}_2(\xi) = \exp\left\{\xi^* \hat{a}\hat{b} - \xi \hat{a}^\dagger \hat{b}^\dagger\right\} \tag{16}$$

Like $\hat{S}$, $\hat{S}_2$ exhibits pairing between creation and annihilation operators. Although, one key difference for $\hat{S}_2$ is that the squeezing is in the quadratures of the two-mode system formed by a superposition of the underlying $\hat{a}$ and $\hat{b}$ quadratures. The underlying $\hat{a}$ and $\hat{b}$ quadratures are

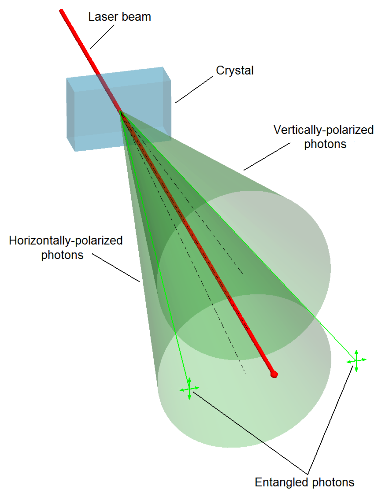

Figure 2. Two-photon squeezed states corresponding to signal and idler beams (green) produced by non-degenerate parametric down conversion in a $\chi^{(2)}$ crystal [9].

not necessarily squeezed. These superposition quadratures are defined as

$$\hat{X}_1^{ab} = \frac{1}{\sqrt{2}}\left(\hat{X}_1^a + \hat{X}_1^b\right) = \frac{1}{2^{3/2}}\left(\hat{a} + \hat{a}^\dagger + \hat{b} + \hat{b}^\dagger\right) \quad (17)$$

$$\hat{X}_2^{ab} = \frac{1}{\sqrt{2}}\left(\hat{X}_2^a + \hat{X}_2^b\right) = \frac{1}{2^{3/2}i}\left(\hat{a} - \hat{a}^\dagger + \hat{b} - \hat{b}^\dagger\right) \quad (18)$$

where the letter superscripts refer to the $\hat{X}_1$ and $\hat{X}_2$ quadratures given by eqs. 3 and 4 for modes a and b [2].

To demonstrate the effect of two-mode squeezing, we again consider the "two-mode squeezed vacuum state" (TMSV): $\hat{S}_2 \left|0,0\right\rangle$. Following a similar procedure as in section I with $\theta = 0$, we again obtain a similar Bogoliubov transformation:

$$\hat{S}_2{}^\dagger \hat{a} \hat{S}_2 = \hat{a}\cosh r - \hat{b}^\dagger \sinh r \quad (19)$$

$$\hat{S}_2{}^\dagger \hat{b} \hat{S}_2 = \hat{b}\cosh r - \hat{a}^\dagger \sinh r \quad (20)$$

The resulting variances of the superposition quadratures calculated with respect to the TMSV have exactly the same form as eqs. 9, 10:

$$\langle(\Delta \hat{X_1^{ab}})^2\rangle = \frac{1}{4}e^{-2r} \quad (21)$$

$$\langle(\Delta \hat{X_2^{ab}})^2\rangle = \frac{1}{4}e^{2r} \quad (22)$$

This squeezing of superposition quadratures implies that some of the underlying a and b quadratures become correlated.

Let us now also interpret the physical significance of the two-mode squeezing operator. The importance of the correlations between photon pairs becomes even more apparent in the case of two-mode squeezing. Most obviously, the Taylor expansion of $\hat{S}_2$

$$\hat{S}_2(\xi) = 1 + \xi^* \hat{a}\hat{b} - \xi \hat{a}^\dagger \hat{b}^\dagger + \frac{1}{2}(\xi^* \hat{a}\hat{b} - \xi \hat{a}^\dagger \hat{b}^\dagger)^2 + ... \quad (23)$$

explicitly reveals that two-mode squeezed states are always acted on by pairs of $\hat{a}\hat{b}$ or $\hat{a}^\dagger\hat{b}^\dagger$. Moreover, one can decompose the TMSV into the number basis by calculating its inner product with coherent states to obtain

$$\hat{S}_2 \left|0,0\right\rangle = \frac{1}{\cosh r}\sum_{n=0}^{\infty}(-1)^n \tanh^n r \left|n,n\right\rangle \quad (24)$$

Evidently, this formulation reveals that the only states which emerge in a superposition to construct the TMSV state are those which are pairs of equal number of photons in the $\hat{a}$ and $\hat{b}$ modes [2].

In addition, $\hat{S}_2$, like $\hat{S}$, can also be viewed as the time-evolution operator to a specific Hamiltonian which is bilinear in the mode operators of the form

$$\hat{H} = i\hbar\chi^{(2)}\left(\hat{a}\hat{b} - \hat{a}^\dagger\hat{b}^\dagger\right) \quad (25)$$

where now, for $\theta = 0$, the time evolution scales as $r = \chi^{(2)}t$. This Hamiltonian again corresponds to a $\chi^{(2)}$ process of parametric downconversion. However, the key distinction between this production mechanism as compared to single-mode squeezed states is that two-mode squeezing require *non-degenerate* parametric downconversion. In this case, $w_2 \neq \frac{1}{2}w_1$ and the signal and idler beams are distinguishable, as shown in figure 2. In fact, any quadratic or bilinear Hamiltonian can produce two-mode squeezing [4, 5]. This arises from the fact that squeezed state wave functions are two-mode Gaussian, and linear transformations on Gaussian states produce other Gaussians [10].

From both single-mode and two-mode squeezed states, we have shown that the physical significance of squeezing is three-fold: *(1)* it always acts on photons in pairs, *(2)* it can be viewed as a dynamical process that can be engineered in a lab, and *(3)* it produces correlations between observable quadratures. These attributes pave the way for a connection between two-mode squeezing and entanglement in the EPR paradox, which we now explore.

II. EPR PARADOX AND TWO-MODE SQUEEZING

A. The EPR Paradox

In a seminal paper in 1935, Einstein, Podolsky, and Rosen (EPR) argued that quantum mechanics leads to a paradoxical result, and therefore cannot be a complete theory [11]. To arrive at this paradox, EPR consider two systems consisting of a single free particle prepared separately by two observers Alice and Bob, which interact for some finite time. The resulting states of the two particles can then be determined when Alice or Bob makes a projective measurement to collapse the two-system wave function onto either of their position or momentum bases.

Suppose Alice makes a position measurement on her particle without disturbing Bob's system. Because the position states of Alice and Bob's particles are assumed to be maximally correlated from their interaction, Alice's measurement will then determine with certainty the position of Bob's particle. Similarly, if Alice had instead made a momentum measurement, then the momentum of Bob's particle would be determined with equal certainty. In other words, the resulting position and momentum wavefunctions of the two-particle system after the measurements yield

$$\Psi(X_a, X_b) = \delta(X_a - X_b) \tag{26}$$

$$\Phi(P_a, P_b) = \delta(P_a + P_b) \tag{27}$$

where the signs are determined by the eigenvalue relations between position and momentum. These are referred to as "EPR states" in contemporary literature [4, 6, 12, 13].

Hence, the arbitrariness in Alice's choice of measurement indicates that Bob's particle has both a definite position and momentum; the above two wavefunctions correspond to the same physical reality. However, according the HUP, this is impossible since position and momentum operators do not commute. Thus, we arrive at a paradox: quantum theory and the philosophical theory of local realism are mutually incompatible. "Locality" refers to the belief that space-like separated events should have no causal impact on each other. "Realism" refers to the belief that observables of physical systems have objective reality and are not measurement-dependent [12].

B. EPR States as Two-Mode Squeezed Vacuum States

Given that the two-mode squeeze states exhibit strong correlations between two distinguishable and non-commuting quadratures, it is natural to ask whether there exists a connection between these states and EPR states. Indeed, the position and momentum operators of both Alice and Bob's system are analogous to the X_1 and X_2 quadratures of the the a and b modes of the TMSV discussed in section I

$$X_a \to X_1^a \tag{28}$$

$$X_b \to X_1^b \tag{29}$$

$$P_a \to X_2^a \tag{30}$$

$$P_b \to X_2^b \tag{31}$$

Let us now consider a different superposition quadrature of the two-mode state defined by the difference of the "position" quadratures

$$\frac{1}{\sqrt{2}}\Big(\hat{X}_1^a - \hat{X}_1^b\Big) = \frac{1}{2^{3/2}}\Big(\hat{a} + \hat{a}^\dagger - \hat{b} - \hat{b}^\dagger\Big) \tag{32}$$

If we compute the variance of this difference superposition quadrature with respect to the TMSV, we obtain a similar form of Bogoliubov transformations which can be viewed as the time-evolution of the non-degenerate parametric downconversion Hamiltonian,

$$\hat{a}(t) = \hat{S_2}^\dagger \hat{a} \hat{S_2} = \hat{a}(0)\cosh r + e^{i\theta}\hat{b}^\dagger(0)\sinh r \tag{33}$$

$$\hat{b}(t) = \hat{S_2}^\dagger \hat{b} \hat{S_2} = \hat{b}(0)\cosh r + e^{i\theta}\hat{a}^\dagger(0)\sinh r \tag{34}$$

where again $r(t) = \chi^{(2)}t$ and θ is left arbitrary here for completeness [2, 4]. To analyze the variance along the position-analog quadratures, we set $\theta = 0$. Substituting the resulting eqs. 33 and 34 into $\hat{S_2}^\dagger \frac{1}{\sqrt{2}}\Big(\hat{X}_1^a - \hat{X}_1^b\Big)\hat{S_2}$, we observe that

$$\frac{1}{\sqrt{2}}\Big(\hat{X}_1^a(t) \pm \hat{X}_1^b(t)\Big) = \frac{1}{\sqrt{2}}\Big(\hat{X}_1^a(0) \pm \hat{X}_1^b(0)\Big)e^{\pm r} \tag{35}$$

where we have also included the time-evolution of the position sum superposition quadrature as well. Similarly, if we set $\theta = \pi$ to determine the variance in the momentum-analog quadratures, a similar calculation produces

$$\frac{1}{\sqrt{2}}\Big(\hat{X}_2^a(t) \pm \hat{X}_2^b(t)\Big) = \frac{1}{\sqrt{2}}\Big(\hat{X}_2^a(0) \pm \hat{X}_2^b(0)\Big)e^{\mp r} \tag{36}$$

Evidently from eqs. 35 and 36, as time evolves (or equivalently as the squeezing parameter r increases) the two-mode squeezing operator correlates the position quadratures and anti-correlates the momentum quadratures of the a and b modes [4]. That is,

$$\langle(\Delta(\hat{X}_1^a - \hat{X}_1^b))^2\rangle = \frac{1}{4}e^{-2r} \tag{37}$$

$$\langle(\Delta(\hat{X}_2^a + \hat{X}_2^b))^2\rangle = \frac{1}{4}e^{-2r} \tag{38}$$

where the opposite signs indicate the correlation and anti-correlation.

For $r(t = 0)$, the above superposition quadratures are uncorrelated. But as $r(t \to \infty)$, they recover the EPR states of eqs. 26, 27; the uncertainty in the difference between the position-analog quadratures and in the sum of the momentum-analog quadratures approaches zero. The EPR states, therefore, are a limiting case of two-mode squeezed states.

This conclusion can also be seen from the wave functions of the TMSV, which are two-mode Gaussian packets. The position wave function is

$$\Psi(x_a, x_b) = \frac{1}{\sqrt{2\pi}}\exp\big(-e^{-2r}(x_a + x_b)^2/4\big)\times \exp\big(-e^{2r}(x_a - x_b)^2/4\big) \tag{39}$$

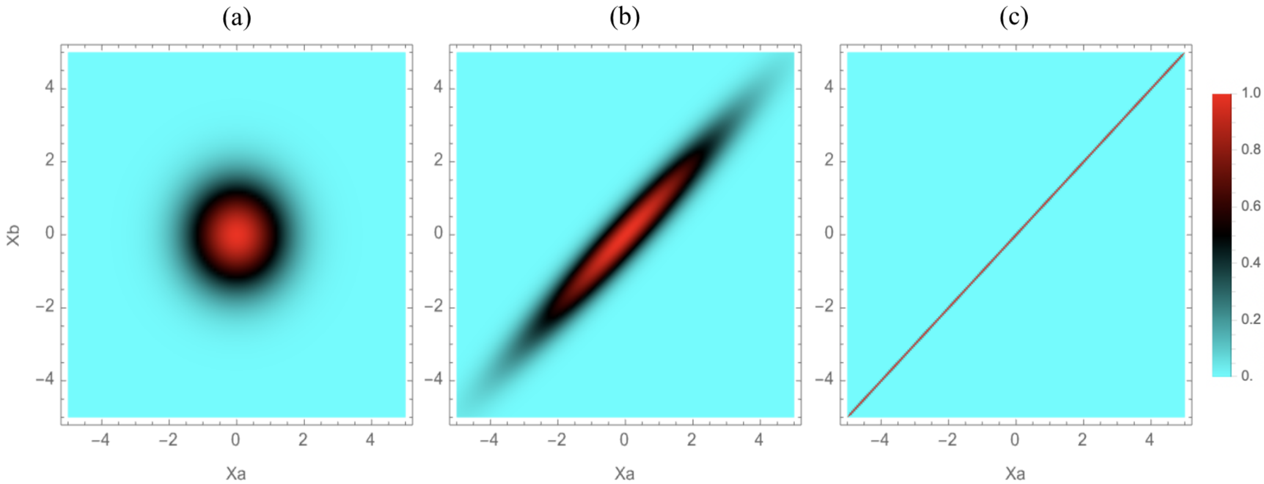

Figure 3. Mathematica simulations of the time-evolution of the TMSV position wavefunction (eq. 39) probability density. At $t = 0$, the state initially begins as the unsqueezed two-mode vacuum state then as the $r(t)$ evolves, x_a and x_b become increasing correlated and the wavefunction recovers the EPR state (eq. 26) as shown for (a) $r = 0$, (b) $r = 1$, and (c) $r = 5$.

where x_a and x_b are the eigenvalues of $\hat{X}_1^a$ and $\hat{X}_1^b$ respectively. Figure 3 shows the evolution of the probability density of TMSV position wave function over time, which exactly approaches the EPR position wave function of eq. 26. The momentum wave function $\Phi(p_a, p_b)$ would exhibit anti-correlation between the momentum-analog quadratures of the TMSV as predicted by the EPR state of eq. 27 as well [4].

In fact, recent studies suggest that any two-mode Gaussian state can be passively transformed to a class of states which saturate a quantity called the "entanglement potential" [10]. Passive transformations refer operations achievable by linear optics, and the entanglement potential is a measure of the highest degree of entanglement from such passive transformations. Li et al. [10] conjecture, therefore, an equivalence between a measure of entanglement potential and a measure of squeezing. This conjecture dictates that the degree of maximal entanglement for a two-mode continuous variable system, such as the EPR states, is entirely determined by the degree of squeezing between those two states. Since the degree of two-mode squeezing can be engineered through non-degenerate parametric down-conversion, this opens the door to manufacturing entangled state in the lab to provide direct tests of the EPR paradox.

C. Experimental Tests of the EPR Paradox Using Squeezed States

The most common production mechanism of the two-mode squeezed states has been non-degenerate parametric downconversion, specifically Type II in which the points of overlap between the signal and idler cones correspond to entangled photons (see Fig. 2) [12, 14]. One method for achieving the high squeezing parameter r necessary for the EPR states is to place $\chi^{(2)}$ crystals back-to-back, as this method has been shown to mitigate the need for phase-matching and produces a homodyne tomography of the reconstructed EPR state with a fidelity of 98% [14]. Methods such as this one have been used to perform tests of the EPR paradox, resulting in the conclusion that local realism is false.

One cornerstone experiment performed by Ou and Mandel [15] was one of the first to explicitly make use of parametric down conversion. Their experimental setup consisted of shining a 351.1 mm argon-ion laser pump beam onto a potassium dihydrogen phosphate nonlinear crystal, and subsequently using a beamsplitter to direct the signal and idler beams onto different photodetectors for coincidence measurements. Any measurement for which $\langle(\Delta\hat{X}_1^a)^2\rangle\langle(\Delta\hat{X}_2^a)^2\rangle \leq 2$ would indicate a violation of local realism and classical probability relations for waves, and their results show a minimal value of 0.7 ± 0.001 [6, 15].

More recently, Zeilinger et al. also used an argon-ion laser pump on a Type II non-degenerate BBO crystal to provide a direct test of another inequality called "Bell's inequality" [16]. Bell's inequality was formulated to provide a concrete experimental measure for testing the EPR paradox [17]. Their setup improved upon a similar experiment by Aspect et al. [18] by closing loopholes such as making the two observers space-like separated. They likewise find a violation of Bell's inequality and therefore local realism.

III. APPLICATIONS OF EPR TWO-MODE SQUEEZING TO METROLOGY

A. LIGO

Beyond providing tests of the nature of quantum mechanics, squeezed light has played a vital role in enhancing quantum sensing precision measurements for fundamental physics. One prime example is the Laser Interferometer Gravitational-Wave Observatory (LIGO), which searches for low-frequency gravitational waves using a 4km Fabry-Perot interferometer [19]. The presence of a gravitational wave perturbs the cavity length in the arms of the interferometer, and this strain force h can be measured with an intensity correlation measurement. To achieve sensitivity to the critical frequency band of around 150-300Hz, LIGO needed operate below the Standard Quantum Limit (SQL), which is the lower limit of their optomechanical HUP relation:

$$\Delta h_{SQL} = \frac{1}{4kl|\alpha|} \tag{40}$$

where $l = 4km$, k is the wave vector, and $|\alpha|$ is the amplitude of the beam [20].

The two main noise sources for gravitational wave interferometers are 1) photon shot noise and 2) radiation pressure noise, which result from fluctuations in the photon counting statistics and the pressure exerted on the cavity mirrors by the field vacuum, respectively. These two noise sources diminish sensitivity to the 1) phase and 2) amplitude quadratures of the interferometer beam. Radiation pressure noise dominates in the high-frequency regime wherein well-motivate astrophysical events occur [20]. As such, LIGO injected single-mode phase-squeezed vacuum produced by a $\chi^{(2)}$ process called Optical Parametric Oscillation (OPO) into the dark port of their interferometer, which improved their high-frequency sensitivity by 2.15dB [19].

To improve upon this result, the newest experimental version called "Advanced LIGO" is employing frequency-dependent squeezing to reduce the uncertainty in the phase quadrature for high-frequencies while reducing uncertainty in the amplitude quadrature for low-frequencies. While still only injecting vacuum squeezed in one quadrature, Advanced LIGO introduces an additional 300m cavity that is detuned from the interferometer resonance in order to filter the injected squeezed vacuum. The filter cavity introduce a phase shift that rotates squeezed states for frequencies detuned from the cavity resonance. The use of frequency-dependent squeezing resulted in a general enhancement of detection efficiency by 15-18% compared to no squeezing as shown in figure 4. However, the addition of of the filter cavity introduced additional optical losses from both cavity losses of the injected squeezed vacuum and readout losses from misalignments in the filtered beam path [21].

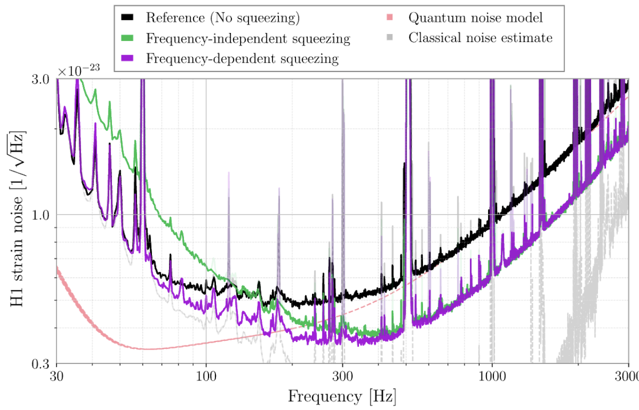

Figure 4. Results of frequency-dependent squeezing in Advanced LIGO [21]. Enhanced sensitivity across the entire parameter space shown in purple for frequency-dependent squeezing.

B. Prospects of EPR Two-Mode Squeezing in Advanced LIGO

At this point, we pause to notice that LIGO has thus-far only implemented single-mode squeezed light. Based on the connection established in section II between EPR states and two-mode squeezed states, we now consider how the use of two-mode squeezing and entanglement could enhance LIGO's frequency-dependent squeezing sensitivity. Instead of introducing an extra cavity, one can prepare a TMSV with correlations tuned to the desired frequency with using non-degenerate Type II parametric down conversion, such as the technique mentioned previously of positioning two $\chi^{(2)}$ crystals back-to-back [14].

Specifically, one can achieve the non-degeneracy by setting the signal mode frequency as w_0 and idler frequency as $w_0 + \Delta$, where $\Delta = \mathcal{O}(MHz)$. This frequency difference produces an entanglement between the resulting sidebands $\pm\Omega$ of the signal and idler modes $\hat{a}$ and $\hat{b}$. These two operators can be characterized according to

$$\hat{a}_{\pm} \rightarrow w_0 \pm \Omega \tag{41}$$

$$\hat{b}_{\pm} \rightarrow w_0 + \Delta \pm \Omega \tag{42}$$

The frequency-shifted idler mode $\hat{b}$ will then see the LIGO interferometer as a detuned cavity and therefore acquire a frequency-dependent rotation set by Δ. Then with two separate homodyne measurements of the signal and idler beams, a measurement on a quadrature of the idler mode will squeeze the corresponding quadrature in the signal mode, in line with the EPR correlations from the two-mode squeezed state. This approach has been referred to as "conditional frequency-dependent squeezing" since the quadrature squeezing in the signal mode is conditional on the measurement outcome on the idler

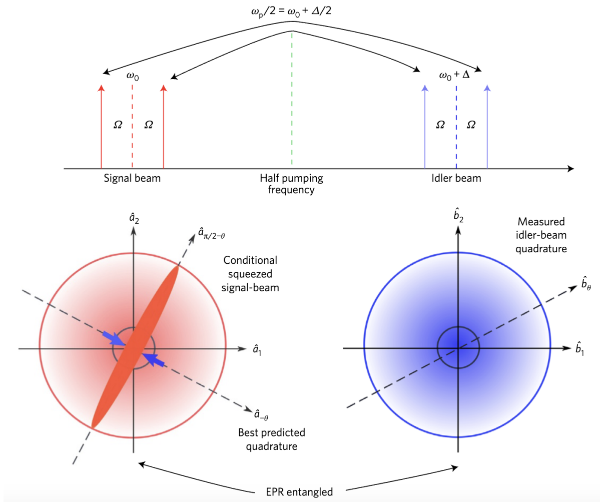

Figure 5. Conditional frequency-dependent EPR squeezing schematic for LIGO. Entanglement is generated between the $w_0 \pm \Omega$ and $w_0 + \Delta \pm \Omega$ side bands of the two-mode squeezed state. A measurement on a quadrature of the idler $\hat{b}$ will squeeze the corresponding quadrature in the signal $\hat{a}$ [13].

mode by an amount of e^{-2r} (see figure 5) [13, 22].

This approach has potential to result in a gain of 11-12dB in sensitivity from the SQL, and an improvement of 6dB on the current Advanced LIGO frequency-dependent method in frequency regions where optical losses are around 5% [13]. The major benefit would be to completely avoid any optical cavity losses that are currently present from using additional filtering cavities to achieve the frequency-dependence. Moreover, one has greater control in tuning the frequency dependence simply by adjusting Δ. However, since the signal and idler modes now require separate homodyne measurements, the read-out optical losses will double. As LIGO collects more data, it will therefore be important to discern which form of optical loss is more prevalent, and if the cavity loss dominates, then the EPR two-mode squeezing approach would improve frequency-dependent squeezing sensitivity [13, 22].

IV. CONCLUSION AND OUTLOOK

By analyzing the physical significance of squeezing, we have demonstrated the profound connection between two-mode squeezing and maximally entangled EPR states. That is, EPR states can be seen as a special case of two-mode squeezed states wherein the squeezing parameter approaches infinity. The fact that two-mode squeezing can be dynamically realized through a $\chi^{(2)}$ nonlinear optical process of non-degenerate parametric down-conversion has enabled direct experimental tests of the foundations of quantum mechanics, and enabled the use of entanglement as a resource to conduct high-precision measurements such as in LIGO.

More generally, generating a network of entangled detectors has promising potential for revolutionizing optomechanical sensing [23]. Demonstrations of an entangled network of table-top cavity optomechanical sensors similar to the style of LIGO have demonstrated a 25% enhancement in detection efficiency compared to classical systems, and specifically a 40% enhancement in reducing shot-noise. According to the central limit theorem, accumulating measurements over M different entangled beams and sensors will reduce the power spectral density by $1/\sqrt{M}$. Accordingly, an array of $M \geq 2$ EPR entangled beams from multi-mode squeezing may be useful to consider for future implementations of LIGO and other force-sensing cavity optomechanics experiments. Future prospects of squeezed state-generated entanglement to search for new fundamental physics should continue to be explored in metrology such as for searching for BSM particles like the axion [23] or sterile neutrino [24], and in future gravitational wave interferometers [22].

* bknepper@berkeley.edu

[1] D. F. Walls, Squeezed states of light, Nature **306**, 141 (1963).
[2] C. C. Gerry and P. L. Knight, *Introductory Quantum Optics*, 2nd ed. (Cambridge University Press, 2024).
[3] A.-D. Zhu, S. Zhang, K. Yeon, S. C. Yu, and U. Chung-In, Creating unconventional geometric phase gate using squeeze-like operator assisted by strong driving field, Chinese Physics **16**, 1559 (2007).
[4] A. I. Lvovsky, Squeezed light, in *Photonics* (John Wiley Sons, Ltd, 2015) Chap. 5, pp. 121–163.
[5] H. P. Yuen, Two-photon coherent states of the radiation field, Phys. Rev. A **13**, 2226 (1976).
[6] D. F. Walls and G. J. Milburn, *Quantum Optics*, 2nd ed. (Springer Berlin, Heidelberg, 2007).
[7] R. Boyd, *Nonlinear Optics*, 4th ed. (Academic Press, 2020).
[8] R. E. Slusher, L. W. Hollberg, B. Yurke, J. C. Mertz, and J. F. Valley, Observation of squeezed states generated by four-wave mixing in an optical cavity, Phys. Rev. Lett. **55**, 2409 (1985).
[9] Wikipedia, Quantum entanglement, .
[10] B. Li, A. Das, S. Tserkis, P. Narang, P. K. Lam, and S. M. Assad, On the equivalence between squeezing and entanglement potential for two-mode gaussian states, Scientific Reports **13**, 11722 (2023).
[11] A. Einstein, B. Podolsky, and N. Rosen, Can quantum-mechanical description of physical reality be considered complete?, Phys. Rev. **47**, 777 (1935).
[12] P. D. Drummond and M. D. Reid, Correlations in nondegenerate parametric oscillation. ii. below threshold results, Phys. Rev. A **41**, 3930 (1990).
[13] Y. Ma, H. Miao, B. H. Pang, M. Evans, C. Zhao, J. Harms, R. Schnabel, and Y. Chen, Proposal for gravitational-wave detection beyond the standard quantum limit through epr entanglement, Nature Physics **13**, 10.1007/s41114-019-0018-y (2017).

[14] I. A. Fedorov, A. E. Ulanov, Y. V. Kurochkin, and A. I. Lvovsky, Synthesis of the einstein–podolsky–rosen entanglement in a sequence of two single-mode squeezers, Optics Letters **42**, 132 (2016).

[15] Z. Y. Ou and L. Mandel, Violation of bell's inequality and classical probability in a two-photon correlation experiment, Phys. Rev. Lett. **61**, 50 (1988).

[16] G. Weihs, T. Jennewein, C. Simon, H. Weinfurter, and A. Zeilinger, Violation of bell's inequality under strict einstein locality conditions, Phys. Rev. Lett. **81**, 5039 (1998).

[17] J. S. Bell, On the einstein podolsky rosen paradox, Physics Physique Fizika **1**, 195 (1964).

[18] A. Aspect, P. Grangier, and G. Roger, Experimental realization of einstein-podolsky-rosen-bohm gedankenexperiment: A new violation of bell's inequalities, Phys. Rev. Lett. **49**, 91 (1982).

[19] J. A. et. al (LIGO Scientific Collaboration), Enhanced sensitivity of the ligo gravitational wave detector by using squeezed states of light, Nature Photonics **7**, 613 (2013).

[20] C. M. Caves, Quantum-mechanical noise in an interferometer, Phys. Rev. D **23**, 1693 (1981).

[21] D. G. et. al (LIGO O4 Detector Collaboration), Broadband quantum enhancement of the ligo detectors with frequency-dependent squeezing, Phys. Rev. X **13**, 041021 (2023).

[22] S. L. Danilishin, F. Y. Khalili, and M. Haixing, Advanced quantum techniques for future gravitational-wave detectors, Living Reviews in Relativity **22**, 10.1007/s41114-019-0018-y (2019).

[23] Y. Xia, A. R. Agrawal, C. M. Pluchar, A. J. Brady, Z. Liu, Q. Zhuang, D. J. Wilson, and Z. Zhang, Entanglement-enhanced optomechanical sensing, Nature Photonics **17**, 10.1038/s41566-023-01178-0 (2023).

[24] D. Carney, K. G. Leach, and D. C. Moore, Searches for massive neutrinos with mechanical quantum sensors, PRX Quantum **4**, 10.1103/prxquantum.4.010315 (2023).